A Dynamical Vector Hysteresis Model Based on an Energy Approach

François Henrotte and Kay Hameyer

Institute of Electrical Machines, RWTH Aachen University, D-52056 Aachen, Germany

A dynamical vector hysteresis model is presented, which is a generalization of a quasistatic model proposed in a recent paper. The model can be considered from the point of view of a mechanical analogy with the pinning of Bloch walls phenomenon represented by a friction force. By combining several elementary submodels with each other, the number of parameter can be increased for a better accuracy.

***Index Terms*—Energy conservation, magnetic energy storage, magnetic hysteresis, magnetic material.**

I. Introduction

THE quality of hysteresis models is generally assessed on basis of their ability to reproduce accurately magnetic b–h curves obtained from measurements. As standard measurements of magnetic characteristics are done along a particular direction (Single sheet tester, Epstein frame), it is not surprising that classical hysteresis models are essentially scalar models. But, if one is interested in the computation of losses or forces in a magnetic material with hysteresis, the ability of matching measured b–h curves is no longer a sufficient proof of the quality of the model. A complete material model is needed, which is able to provide the different terms of the local energy balance in the material and from which constitutive laws can be derived consistently.

Preisach's model [1], for instance, has no interpretation in terms of energy, and further assumptions need have to be done to estimate instantaneous losses [2], [3]. On the other hand, the basic assumptions of the Jiles–Atherton model [4] constitute a true material model with an interpretation in terms of energy. However, at a certain point in the development of the model, algebraic and differential operations are performed, which make loose track of the grounding energy concepts. At the end, the model does not generalize naturally to two or three dimensions of space. Nor provides it any more an energy balance of the material.

In a recent paper [5], an alternative quasistatic hysteresis model has been proposed, which like the Jiles–Atherton model, is based on the representation of magnetic hysteresis by a friction-like force. This model, which has similarities with the model proposed by Bergqvist [6], [7], remains however all through consistent with a genuine energy interpretation of the magnetic material's behavior. This model is also intrinsically a vector model and it needs therefore not to be explicitly vectorized. In this paper, a dynamical term is added to the quasistatic model presented in [5], so as to obtain a dynamical vector model.

II. Physics of Ferromagnetism

A. Magnetic Polarization

Magnetic materials, in general, are characterized by the existence of permanent atomic magnetic moments of amplitude m_o [A·m^2], which are free to rotate, and to orient in space, in function of several external and internal factors (applied field, crystallographic structure, thermal agitation, etc.).

Now let $\mathbf{h}_r$ be the magnetic field along a given direction, say $\mathbf{h}_r = h_r \mathbf{e}_{\mathbf{h}_r}$, with the notations $x \equiv |\mathbf{x}|$ end $\mathbf{e}_\mathbf{x} \equiv \mathbf{x}/x$. Each individual magnetic moment can be associated an angle θ with respect to the field and an energy $\Psi(\theta) = -\mu_0 m_o h_r \cos\theta$. The macroscopic magnetization $\mathbf{M}$ of the sample is obtained by a statistical approach assuming a Boltzmann distribution

$$\mathbf{M}(\mathbf{h}_r) = M_s L\left(\frac{h_r}{h_s}\right)\mathbf{e}_{\mathbf{h}_r}, \quad L(x) = \coth x - \frac{1}{x} \tag{1}$$

with $M_s[T]$ the saturation magnetization, $h_s = k_B T/(\mu_0 m_o)$ a characteristic field, and L the Langevin function (see, e.g., [9] for details).

B. Ferromagnetism

The magnetization of ferromagnetic monocrystals (Fe, Ni, Co, etc.) is explained by the presence of a strong short-range force of quantum origin. Due to that supplementary interaction, the atomic moments not only tend to align with the applied field, but tend also to remain all parallel with each other. Because of the anisotropy of the crystal lattice, they moreover align preferably along a limited set of particular directions, called directions of easy magnetization of the crystal.

A very strong magnetic field would be associated with the situation where all magnetic moments are parallel with each other. In order to minimize the magnetic energy of the sample, the field lines associated with that strong field close themselves preferably inside the magnetic material, so that the sample divides itself spontaneously, at a mesoscopic scale, into a large number of small regions called Weiss domains, where all moments are parallel to each other. In practice, one has often to deal with polycrystalline materials, which are agglomerates of monocrystals oriented evenly in all directions, so that the anisotropy properties of individual monocrystals are averaged out. In such conditions, the statistical approach of the previous section is still valid, and the macroscopic magnetization of the polycrystal can be described by (1).

C. Magnetic Hysteresis

Two Weiss domains are separated by a transition region, called Bloch wall, where the orientation of the moments varies smoothly from the orientation of the domain on the one side to the one of the domain on the other side. Magnetization of a ferromagnetic material implies the motion of walls. The

Digital Object Identifier 10.1109/TMAG.2006.872473

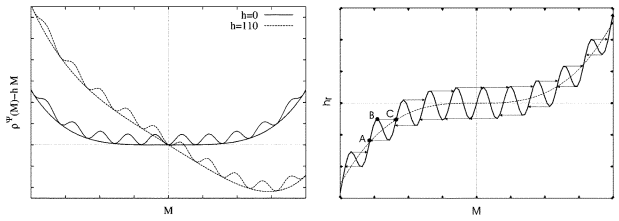

Fig. 1. (a) On the left, energy density functionals $\rho^{\Psi}(\mathbf{M}) - \mathbf{h} \cdot \mathbf{M}$ without (nonrippled) and with inclusions (rippled) in the crystal lattice. (b) On the right, the corresponding internal magnetic field $\mathbf{h}_r \equiv \partial_{\mathbf{M}} \rho^{\Psi}$. The arrows represent the Barkhausen jumps.

reversibility of the magnetization process depends on the presence or not of inclusions and impurities in the crystal lattice. Without inclusions, the magnetic energy density functional $\rho^{\Psi}(\mathbf{M})$ looks like the nonrippled solid curve in Fig. 1(a). It has one single minimum, at $\mathbf{M} = 0$.

In the presence of an applied field $\mathbf{h}$, the magnetization is the minimum of the functional $\rho^{\Psi} - \mathbf{h} \cdot \mathbf{M}$, i.e., the nonrippled dotted curve in Fig. 1(a). In the one-dimensional case, it can also be determined graphically as the intersection of the curve $h_r \equiv \partial_{\mathbf{M}} \rho^{\Psi}$ [dotted nonrippled curve in Fig. 1(b)] with an horizontal line at h. In a perfect crystal, i.e., without defects, the intersection is unique for all h and magnetization goes smoothly. This means the walls move freely and there is no dissipation associated with a quasistatic variation of the applied field. Note carefully that rapid variations of $\mathbf{h}$ would however generate local eddy currents in the wall, and therefore Joule losses. This contribution will be represented separately in the model.

In the presence of inclusions, the energy density is like the rippled curve in Fig. 1(a). Such defects constitute indeed small amagnetic voids in the crystal structure. They pin the Bloch walls at fixed positions because the energy density presents a local minimum whenever a wall crosses an inclusion. The magnetization is again determined by intersecting a horizontal line at h with the curve $h_r(M)$ in Fig. 1(b). At h located just below h_A, there is one intersection. One has, between h_A and h_B, a region with three intersections. Two of them are stable (positive slope) and one is unstable (negative slope). However, by continuity, the actual magnetization is the intersection with the flank $A - B$. At B, the pinning force $h_r(M_B)$ is not able any more to withstand the applied field $h = h_B$ and the Bloch wall jumps to the next pinning site where a sufficient pinning force is found, i.e., in C. This sudden move of the wall is associated with a jump of $\mathbf{M}$, which generates eddy currents and dissipates, by Joule effect, the amount of energy represented by the area of the curvilinear quadrangle delimited by the segment BC and the curve $h_r(M(t))$. However the rate of this dissipation, which we shall call quasistatic, is related with the dynamics of the wall motion, and not with the rate of variation of the applied field $\dot{\mathbf{h}}$. The two contributions, quasistatic and dynamic, are therefore represented separately in this hysteresis model, by the terms in κ and λ, as shown further. More accurately, the power dissipated by the Barkhausen effect writes $(h(t) - h_r(M(t)))\dot{M}(t)$.

At the macroscopic scale, the microscopic distribution of pinning site cannot be represented explicitly and an homogenization is done. The wave number of the energy ripple in increased $\to \infty$, holding the amplitude κ constant, so that, as in the model of Jiles–Atherton, the pinning effect can finally be represented by a frictional force of constant magnitude κ that impedes the motion of Bloch walls and opposes to any magnetization change [4], [8]. The associated work $-\kappa|\dot{\mathbf{M}}|$ is entirely converted into heat.

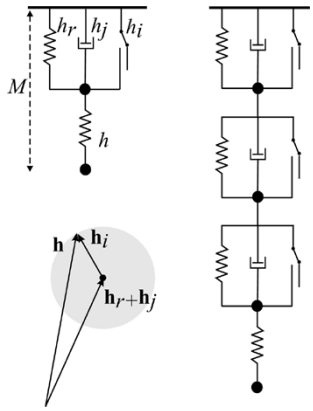

Fig. 2. Mechanical analogy (elementary cell and combined model) and pictorial representation of the vector equilibrium equation (5) of one cell. The grey circle represents the subgradient G.

III. Analogy

After having clarified how the pinning effect can be represented by a friction force, the proposed dynamic hysteresis model can be introduced in terms of a mechanical analogy. An object free to slide on a rough surface and attached with a spring to a fixed point P is considered. The whole system is plunged in a viscous liquid. The position of the object is denoted by the vector $\mathbf{M}$, $\dot{\mathbf{M}}$ is the velocity. Inertia plays no role in the analogy. The differential equation ruling this system can be obtained by a functional approach based on the first principle of Thermodynamics, $\dot{\rho}^{\Psi} = \dot{\rho}^{W} + \dot{\rho}^{Q}$, here written in terms of power densities. The internal energy is the energy stored in the spring. It is a differentiable singled valued function $\rho^{\Psi} : \mathbf{M} \mapsto \mathbb{R}$, which will be assumed to be such that

$$\dot{\rho}^{\Psi}(\mathbf{M}) = \mathbf{h}_r \cdot \dot{\mathbf{M}} \quad \text{with } \mathbf{h}_r = \partial_{\mathbf{M}} \rho^{\Psi}(\mathbf{M}). \tag{2}$$

The power developed by the external force $\mathbf{h}$ writes $\dot{\rho}^{W} = \mathbf{h} \cdot \dot{\mathbf{M}}$. The dissipation functional $\dot{\rho}^{Q} = -\kappa\,|\dot{\mathbf{M}}| - \lambda \dot{\mathbf{M}}^2$ accounts respectively for the dissipation due to friction and the dissipation due to viscosity. As the first principle, now written

$$\mathbf{h}_r \cdot \dot{\mathbf{M}} = \mathbf{h} \cdot \dot{\mathbf{M}} - \kappa|\dot{\mathbf{M}}| - \lambda \dot{\mathbf{M}}^2 \tag{3}$$

must be verified at any time and whatever the trajectory of the object, the equilibrium equation is found by factorizing $\dot{\mathbf{M}}$.

The dissipation functional $\kappa|\dot{\mathbf{M}}|$, however, is not differentiable at $\dot{\mathbf{M}} = 0$. But, as it is convex, it has a subgradient G defined by

$$G = \{\mathbf{h}_i, |\mathbf{h}_i| \leq \kappa \text{ if } \dot{\mathbf{M}} = 0, \mathbf{h}_i = \kappa\, \mathbf{e}_{\dot{\mathbf{M}}} \quad \text{if } \dot{\mathbf{M}} \neq 0\} \tag{4}$$

and represented by the grey circle in Fig. 2. The equilibrium equation writes finally

$$\mathbf{h} - \mathbf{h}_r - \mathbf{h}_j = \mathbf{h}_i \in G \tag{5}$$

with $\mathbf{h}_j \equiv \lambda \dot{\mathbf{M}}$.

The mechanical model can be directly translated into an analogous model for ferromagnetic materials with hysteresis. The vector $\mathbf{M}$ is the magnetization of the material (in Tesla). The

applied force $\mathbf{h}$ is the magnetic field. The friction force $\mathbf{h}_i$ originates from the quasistatic dissipation associated with the pinning of Bloch walls, and the viscosity force $\mathbf{h}_j$ is associated with the local dynamic dissipation by Joule losses. Both dissipative forces have the dimensions of a magnetic field.

The memory effect originates from the nondifferentiable character of the functional $|\dot{\mathbf{M}}|$, which implies the nonunivocity of the friction force $\mathbf{h}_i$. The subgradient is indeed a set of possible gradients (i.e., of possible forces $\mathbf{h}_i$), whereas a differentiable functional has one and only one gradient at each point. If the tip of $\mathbf{h}$ is inside the circle, one has by (4) $\dot{\mathbf{M}} = 0$, which implies by (1) $\dot{\mathbf{h}}_r = 0$. In this way, a given magnetization $\mathbf{M}$ can persist when the magnetic field $\mathbf{h}$ has decreased, whence the memory effect.

If on the contrary the tip of $\mathbf{h}$ tends to get out of the circle, the magnetization is updated according to the differential equation in time

$$\mathbf{h} - \mathbf{h}_r - \mathbf{h}_j = \kappa \mathbf{e}_{\dot{\mathbf{h}}_r} \tag{6}$$

where we have noted that $\mathbf{e}_{\dot{\mathbf{M}}} = \mathbf{e}_{\dot{\mathbf{h}}_r}$. The magnetization $\mathbf{M}$ is obtained by (1), and the induction is $\mathbf{b}(\mathbf{h}) = \mathbf{M}(\mathbf{h}_r) + \mu_0(1+\chi)\mathbf{h}$.

IV. Implementation

Like all hysteresis models, this model fits naturally into a magnetic field formulation. as the latter is the input quantity to the model. In practice, a simplified efficient update rule for $\mathbf{h}_{rj} \equiv \mathbf{h}_r + \mathbf{h}_j$, as the unknown field $\mathbf{h}$ varies, is

$$\left|\mathbf{h}^{n+1} - \mathbf{h}^n_{rj}\right| > \kappa \Rightarrow \mathbf{h}^{n+1}_{rj} = \mathbf{h}^{n+1} - \kappa \frac{\mathbf{h}^{n+1} - \mathbf{h}^n_{rj}}{\left|\mathbf{h}^{n+1} - \mathbf{h}^n_{rj}\right|}, \tag{7}$$

which ensures $|\mathbf{h}_i| = |\mathbf{h} - \mathbf{h}_{rj}| \leq \kappa$ at all time steps, but verifies only approximately (6). If one notes that

$$\partial_t |\mathbf{x}| = \mathbf{e}_{\mathbf{x}} \cdot \partial_t \mathbf{x}, \quad \partial_t \mathbf{e}_{\mathbf{x}} = \frac{\mathbb{I} - \mathbf{e}_{\mathbf{x}}\mathbf{e}_{\mathbf{x}}}{|\mathbf{x}|} \cdot \partial_t \mathbf{x}, \tag{8}$$

one obtains

$$\begin{aligned}\dot{\mathbf{M}} &\equiv \partial_t \left\{M(h_r) e_{\mathbf{h}_r}\right\} = \frac{\partial M}{\partial h_r}(h_r)(\partial_t h_r) e_{\mathbf{h}_r} + M(h_r)\partial_t e_{\mathbf{h}_r} \\ &= \left\{\frac{M(h_r)}{h_r}\mathbb{I} + \left(\frac{\partial M}{\partial h_r}(h_r) - \frac{M(h_r)}{h_r}\right)\mathbf{e}_{\mathbf{h}_r}\mathbf{e}_{\mathbf{h}_r}\right\} \cdot \partial_t \mathbf{h}_r \\ &\equiv \frac{\partial \mathbf{M}}{\partial \mathbf{h}_r}(h_r) \cdot \partial_t \mathbf{h}_r.\end{aligned}$$

The update rule for $\mathbf{h}_r$, knowing $\mathbf{h}^{n+1}_{rj}$, is readily obtained by solving for $\mathbf{h}^{n+1}_r$ the relation

$$\mathbf{h}^{n+1}_{rj} = \mathbf{h}^{n+1}_r + \mathbf{h}^{n+1}_j \approx \mathbf{h}^{n+1}_r + \lambda \frac{\partial \mathbf{M}}{\partial \mathbf{h}_r}(h^n_r) \frac{\mathbf{h}^{n+1}_r - \mathbf{h}^n_r}{\Delta t}. \tag{9}$$

One sees that the nondifferentiable character of the dissipation functional is only a theoretical problem. It amounts to a simple test in (7), i.e., a if-statement in the implementation. With first order shape functions, the unknown field $\mathbf{h}$ is constant in each element and the hysteresis algorithm requires to store the value of the vector $\mathbf{h}_r$ and $\mathbf{h}_{rj}$ for each ferromagnetic element. As the update rule is a vector relation, it gives as such a vector hysteresis model, without making any other assumption.

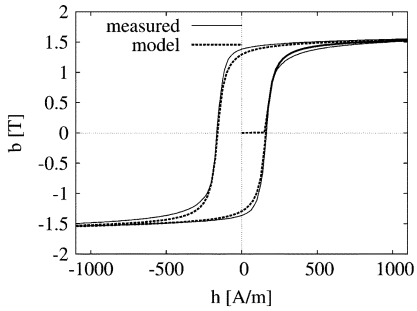

Fig. 3. Measurement and model for steel with the uniaxial quasistatic model.

V. Combined Model

In the form presented so far, the model has only five parameters: M_s, h_s, and χ to represent the anhysteretic curve, κ and λ to represent hysteresis. Although it gives yet qualitatively interesting results for the main hysteresis loop (Fig. 3), a better representation of the material behavior requires to dispose of a larger number of free parameters, which can be achieved as follows.

The idea is to decompose the magnetization $\mathbf{M}$ into different fractions $\mathbf{M}^k$ that are subjected to friction forces of different amplitudes κ^k. Let $\omega^k, k = 0, \ldots, n$ with $\sum_{k=0}^n \omega^k = 1$ being the fraction coefficients, so that $\mathbf{M}^k \equiv \omega^k \mathbf{M}$. For each fraction, one states that (5) remains valid, i.e.,

$$\mathbf{h} = \mathbf{h}^k_{rj} + \mathbf{h}^k_i, \quad k = 0, \ldots, n. \tag{10}$$

This amounts to connect in series several hysteresis cells having each a different value of κ, Fig. 2. The energy balance of the fractions writes

$$\mathbf{h} \cdot \dot{\mathbf{M}}^k = \mathbf{h}^k_{rj} \cdot \dot{\mathbf{M}}^k + \mathbf{h}^k_i \cdot \dot{\mathbf{M}}^k \tag{11}$$

and making the sum on k, one obtains the global energy balance

$$\mathbf{h} \cdot \dot{\mathbf{M}} = \left(\sum_{k=0}^n \omega^k \mathbf{h}^k_{rj}\right) \cdot \dot{\mathbf{M}} + \left(\sum_{k=0}^n \omega^k \mathbf{h}^k_i\right) \cdot \dot{\mathbf{M}} \tag{12}$$

from which follows

$$\mathbf{h} = \sum_{k=0}^n \omega^k \mathbf{h}^k_{rj} + \sum_{k=0}^n \omega^k \mathbf{h}^k_i, \quad \mathbf{h}^k_i \in G^k. \tag{13}$$

The algorithm of the elementary model is applied to each fraction independently, taking for each fraction the particular value of the friction force κ^k into account. Then, the magnetization $\mathbf{M}$ is obtained by (1), with $\mathbf{h}_r = \sum_{k=0}^n \omega^k \mathbf{h}^k_r$. The dissipated power is $\left(\sum_{k=0}^n \omega^k \mathbf{h}^k_i\right) \cdot \dot{\mathbf{M}}$.

The combined model with $n+1$ fractions has $2n+5$ parameters: M_s, h_s, and χ for the anhysteretic curve; λ for the dynamic dissipative term, $\kappa^k, k = 0, \ldots, n$ and $\omega^k, k = 1, \ldots, n$. It is relevant to reserve a fraction with a zero friction force, say $\kappa^0 = 0$. The reversible magnetization $\omega^0 \mathbf{M}$ associated with this fraction represents the bending of the Bloch walls. The combined model requires to store per element the value of the $2n$ vectors $\mathbf{h}^k_r$ and $\mathbf{h}^k_{rj}$.

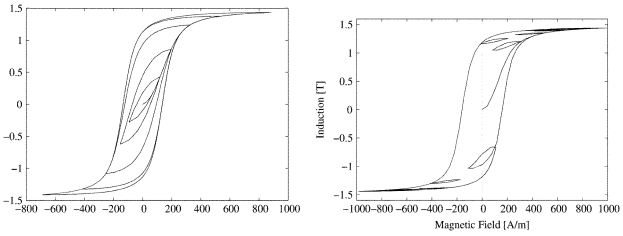

Fig. 4. Internal loops (left) and minor loops (right) are represented by the model.

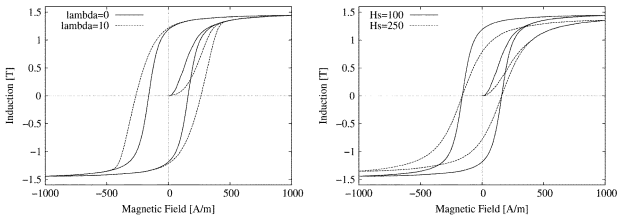

Fig. 5. Effect of the parameters λ and h_s.

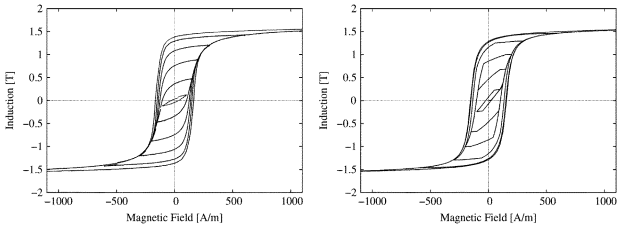

Fig. 6. Measurements (left) and model (right) obtained with five cells for electrical steel.

This model is able to represent internal loops and minor loops, Fig. 4. It exhibits the memory effect and the wiping-out property [1]. The effect of the parameters h_s and λ are represented in Fig. 5. The identification of the parameters has been described in detail for the quasistatic uniaxial case in [5]. The parameters M_s, h_s and χ, are first fitted with the measured anhysteretic curve. Then, the κ^k's are fixed in order to match internal symmetrical loops. Fig. 6 shows the agreement obtained with five cells. The dynamic parameter λ is finally determined on basis of losses measurements at different frequencies. As this hysteresis model is based on a real physical description of the phenomenon, it makes sense to use it in a 3-D model, even whenthough the parameter identification has been done on basis of uniaxial quasistatic measurements.

The model is also able to represent rotational hysteresis, as shown in Fig. 7 for different kind of elliptical applied magnetic fields. Fig. 8 shows the losses computed with a uniaxial applied field, a purely rotational applied field and an elliptical field. One sees the rotational hysteresis losses are about 70% larger than the uniaxial losses.

VI. Conclusion

Unlike the Jiles–Atherton model, for which the magnetization $\mathbf{M}$ is decomposed into a reversible and an irreversible part, the applied field $\mathbf{h}$ is in this model decomposed into a reversible part $\mathbf{h}_r$ and an irreversible part $\mathbf{h}_i + \mathbf{h}_j$. Unlike the models of Preisach and Jiles–Atherton, this model is readily vectorial and dynamic. Moreover, it relies consistently on an energy balance, of which all terms (stored magnetic energy, dissipated energy) are known at all times. Unlike the model of Jiles–Atherton,

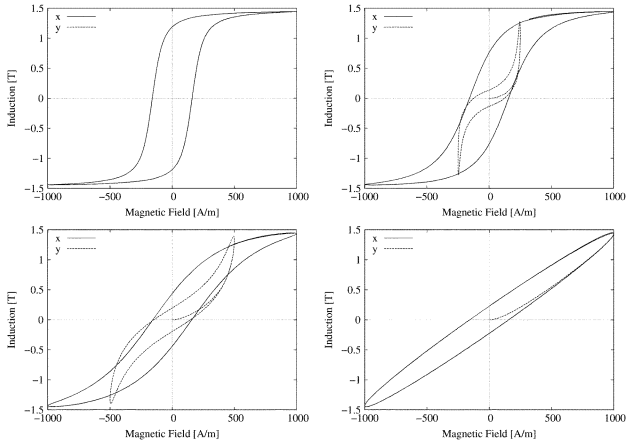

Fig. 7. Rotational hysteresis with $h_x = 1000\cos(\omega t)$ A/m and $h_y = 0, 250, 500$, and $1000\sin(\omega t)$ A/m.

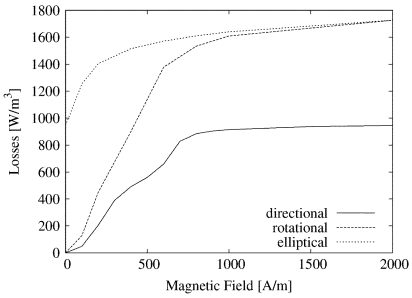

Fig. 8. Rotational losses computed with a uniaxial applied field ($h_y = 0$), purely rotational applied fields (h_x=h_y) and elliptical fields (h_x=1000 A/m).

the number of parameters is not limited. The combined model offers an arbitrary number of parameters. However, due to internal constraints in the model, not all hysteresis curves can be matched exactly. Such a limitation is comparable with the congruence property of the Preisach model [1]. Many ways exist, however, to further develop this model. One may for instance think of adapting functional based elasto-visco-plastic models from Mechanics.

References

[1] I. Mayergoyz, *Mathematical Models of Hysteresis*. New York: Springer-Verlag, 1991.

[2] G. Friedman and I. Mayergoyz, "Hysteretic energy losses in media described by vector Preisach model," *IEEE Trans. Magn.*, vol. 34, no. 4, pp. 1270–1272, Jul. 1998.

[3] F. Delincé, A. Nicolet, A. Genon, and W. Legros, "Analysis of ferroresonace with a finite element method taking hysteresis into account," *J. Magn. Magn. Mater.*, vol. 133, pp. 557–560, 1994.

[4] D. C. Jiles and D. L. Atherton, "Theory of ferromagnetic hysteresis," in *Journal of Magnetism and Magnetic Materials*. Amsterdam, The Netherlands: North-Holland, 1986, vol. 61, pp. 48–60.

[5] F. Henrotte, A. Nicolet, and K. Hameyer, "An energy-based vector hysteresis model for ferromagnetic model," in *Selected Papers from the EPNC'2004 Symp.*, Poznan, Poland, Jun. 28–30, 2004.

[6] A. Bergqvist, "Magnetic vector hysteresis model with friction-like pinning," *Physica B*, vol. 233, pp. 342–347, 1997.

[7] A. Bergqvist, A. Lundgren, and G. Engdahl, "Experimental testing of an anisotropic vector hysteresis model," *IEEE Trans. Magn.*, vol. 33, no. 5, pp. 4152–4154, Sep. 1997.

[8] D. C. Jiles and D. L. Atherton, "Ferromagnetic hysteresis," *IEEE Trans. Magn.*, vol. 19, no. 5, pp. 2183–2185, Sep. 1983.

[9] M. J. Sablik and D. C. Jiles, "Coupled magnetoelastic theory of magnetic and magnetostrictive hysteresis," *IEEE Trans. Magn.*, vol. 29, no. 4, pp. 2113–2123, Jul. 1993.

Manuscript received June 20, 2005 (e-mail: francois.henrotte@iem.rwth-aachen.de).